

Molecular modelling studies on the ORL1-receptor and ORL1-agonists

Britta M. Bröer, Marion Gurrath & Hans-Dieter Höltje*

Institute for Pharmaceutical Chemistry, Heinrich-Heine-University Düsseldorf, Universitätsstrasse 1, D-40225 Düsseldorf, Germany

Received 11 June 2003; accepted in revised form 31 October 2003

Key words: binding site, docking, 3D-QSAR, GPCR, molecular modelling, ORL1-receptor, pharmacophore, receptor model

Summary

The ORL1 (opioid receptor like 1)- receptor is a member of the family of rhodopsin-like G protein-coupled receptors (GPCR) and represents an interesting new therapeutical target since it is involved in a variety of bio-medical important processes, such as anxiety, nociception, feeding, and memory. In order to shed light on the molecular basis of the interactions of the GPCR with its ligands, the receptor protein and a dataset of specific agonists were examined using molecular modelling methods. For that purpose, the conformational space of a very potent non-peptide ORL1-receptor agonist (Ro 64-6198) with a small number of rotatable bonds was analysed in order to derive a pharmacophoric arrangement. The conformational analyses yielded a conformation that served as template for the superposition of a set of related analogues. Structural superposition was achieved by employing the program FlexS. Using the experimental binding data and the superposition of the ligands, a 3D-QSAR analysis applying the GRID/GOLPE method was carried out. After the ligand-based modelling approach, a 3D model of the ORL1-receptor has been constructed using homology modelling methods based on the crystal structure of bovine rhodopsin. A representative structure of the model taken from molecular dynamics simulations was used for a manual docking procedure. Asp-130 and Thr-305 within the ORL1-receptor model served as important hydrophilic interaction partners. Furthermore, a hydrophobic cavity was identified stabilizing the agonists within their binding site. The manual docking results were supported using FlexX, which identified the same protein-ligand interaction points.

Introduction

The superfamily of G protein-coupled receptors (GPCRs) still represents the majority of current drug targets. In 1994, the ORL1-receptor (also called nociceptin/orphaninFQ (N/OFQ)-receptor), a rhodopsin-type GPCR has been discovered [1]. In the course of time, the name of the protein changed (ORL1-, N/OFQ-, OP4-, NOP-receptor) and different denotations were used by diverse working groups. Within this work, the original naming ORL1-receptor was chosen.

After cloning of the cDNA of the μ -, δ - and κ -types, oligonucleotide probes were employed to

screen cDNA libraries, thus identifying a fourth cDNA sequence encoding a previously unknown receptor protein, whose primary structure was revealed to be typical for GPCRs. This receptor is present in all regions of the brain and in the spinal cord. The ORL1-receptor exhibits a significant degree of sequence identity with other opioid receptors, in particular the third cytoplasmatic loop suggests that ORL1-receptor is capable of activating the same G proteins when compared to the opioid receptors. Despite this sequence similarity, the pharmacological implications are different. Because of its wide distribution, it is suggested that the ORL1-receptor plays an important role in many central processes, in particular learning and memory, attention and emotions, movement and motoric processes, homeostasis, neuroendocrine se-

*To whom correspondence should be addressed. E-mail: hoeltje@pharm.uni-duesseldorf.de

cretions and several perceptions [2–4]. The physiological agonist orphanin FQ/nociceptin (N/OFQ) [5], a 17-amino acid neuropeptide (FGGFTGARKSARK-LANQ), acts inhibitory on synaptic transmission in the CNS and thereby contributes e.g. to a reduction in responsiveness to stress and evokes anxiolytic effects [6].

Due to these effects, agonists for the ORL1-receptor may offer interesting possibilities for selective normalization of stress-related neuronal dysfunction or anxiety caused diseases. Consequently, it is of prime importance to derive detailed information about the receptor, its non-peptide ligands, and the corresponding binding pocket within the receptor protein.

Methods

All molecular modelling techniques that are described herein were performed on Silicon Graphics O2 R12000 workstations.

Agonist structure generation

The examined compounds were constructed employing the Sketch routine within SYBYL 6.8 (Tripos, Inc., St. Louis, MO). All molecules were assumed to be mono-protonated under physiological conditions and their molecular structures were generated accordingly. No solvent was taken into account. Energy minimization was carried out applying the TRIPOS force field.

Conformational analysis

The structures and the biological activities of the 25 agonists were taken from literature [7, 8]. The conformational analysis of these structures was performed using SYBYL 6.8 taking compound Ro 64-6198 ($pK_i = 9.41$) (Figure 1) because of its putative small conformational space as a template. For this purpose a low energy structure of Ro 64-6198 had to be determined by a common practice. The ligand was divided into N,N-dimethyl substituted hexahydro-1*H*-phenalen-1-yl (part 1) and phenyl-1,3,8-triazaspiro[4.5]decan-4-one (part 2) to analyse the geometry of the tricyclic system separately from the entire structure. Part 1 was subjected to a simulated annealing protocol: 10 cycles, heating up the system to 2000 K in 1000 fs, respectively, annealing subsequently to 0 K in 2000 fs. The set of conformations generated

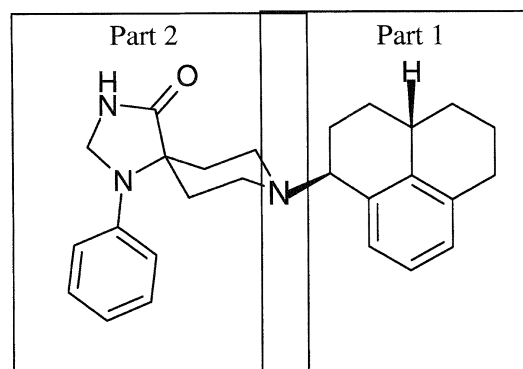


Figure 1. Ro 64-6198 ($pK_i = 9.41$), divided into two substructures for which the conformational space were investigated separately.

showed insignificant variations only. Due to this fact, the conformation with the lowest energy was chosen from the 10 resulting structures. A crystal structure retrieved from the Cambridge Structural Database [9] (FBPAZD01) was utilised (after energy minimization) to construct part 2. After combining both parts, a systematic search was accomplished on the single bond between the ring system and the piperidine (10° steps). This standard procedure yielded a low energy conformation that was used as a reference for the remaining compounds (Figure 2).

Superposition

FlexS [10], a method for fast flexible ligand superposition was used to overlay all other agonists with the given reference. The ligand superimposed onto the template is treated as flexible, while the reference ligand is kept rigid in the assumed bioactive conformation. In essence, the strategy of FlexS is to decompose the flexible ligand into small and relatively rigid portions (fragments), to start the placement with a defined anchor fragment (base fragment and base placement, respectively), and, subsequently, to add the remaining fragments in a stepwise manner (incremental construction) taking conformational degrees of freedom into account. The key algorithms and physicochemical models involved have been described elsewhere in detail [10, 11]. The FlexS algorithm is a modification of the flexible docking algorithm in FlexX (see below).

3D-QSAR analysis

The GRID/GOLPE method was used within this study to perform a 3D-QSAR analysis [12, 13]. In a first step, the molecules were placed into a rectangular grid

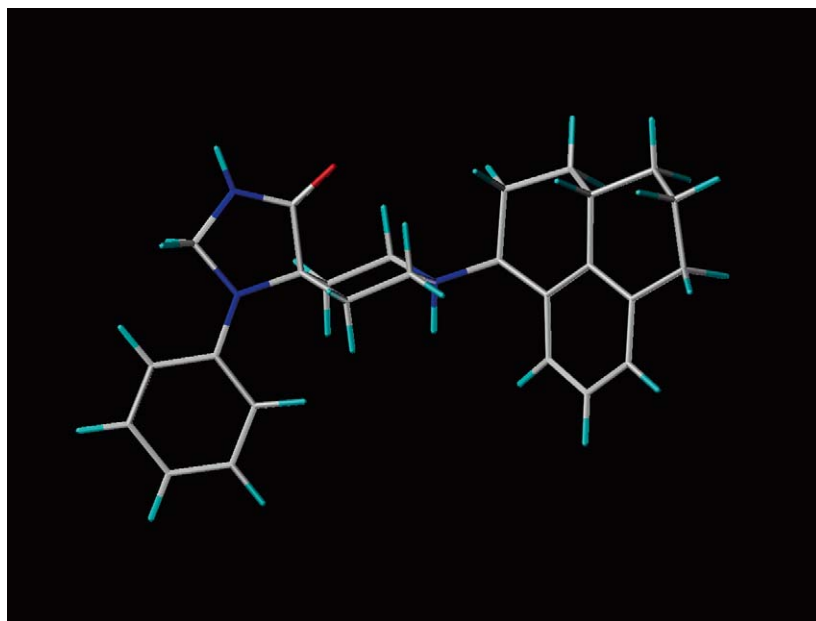


Figure 2. Proposed bioactive conformation of Ro 64-6198.

cage measuring $18 \times 26 \times 17 \text{ \AA}$, applying an 1 \AA spacing, and scanned using a small chemical group (probe) yielding molecular interaction energy values. The size of the grid box considered for the calculation was defined in such a way that it extended approximately 4 \AA beyond each of the molecules in each dimension. The phenolic OH-probe, a polar group with the ability to participate in H-bonds was selected for this study. In order to eliminate the redundant variables that introduced only noise in the statistical PLS analysis [14], the advanced pretreatment procedure, the D-optimal preselection and the SRD/FFD (Smart Region Definition/Fractional Factorial Design) variable selection within the GOLPE program (for a detailed description of this approach, see [14–16]) were employed. Models obtained applying variable selection are in general of higher quality than models calculated without variable selection. In order to obtain a correlation between interaction energy values and the experimental binding data, a Partial Least Square (PLS)-model was generated and validated by the leave-one-out (LOO) and leave-20%-out (L20%O) method (= cross-validation procedures). These statistical analyses were also accomplished by the program GOLPE. The evaluation of the predictivity of the PLS-model is important to assess its quality. The optimum number of PLS components corresponding to the smallest standard error of prediction, was determined by the LOO procedure. Using the optimal number

of components, the final PLS analysis was carried out without cross-validation to generate a predictive model with a conventional correlation coefficient. The LOO cross-validation method might lead to high q^2 values which do not necessarily reflect a general predictiveness of a model. Due to the lack of an adequate external test set, a more robust cross-validation technique, the leave-20%-out method was performed. In this method, 20% of the compounds were randomly selected and a model is generated based on the remaining 80% of the compounds, which is then used to predict the randomly selected compounds (L20%O). This cross-validation technique has been shown to yield better indices for the robustness of a model than the normal LOO procedure [17].

In addition, the dataset was subjected to a scramble test, a commonly accepted method [18, 19] to check whether the obtained correlation had been generated by chance or can be considered as reasonable. The binding affinities of the ligands were scrambled and randomly assigned to the compounds. A PLS model was generated and the variables were reduced as mentioned above. The final PLS-model was validated applying the LOO method. Ten models with scrambled binding data were set up.

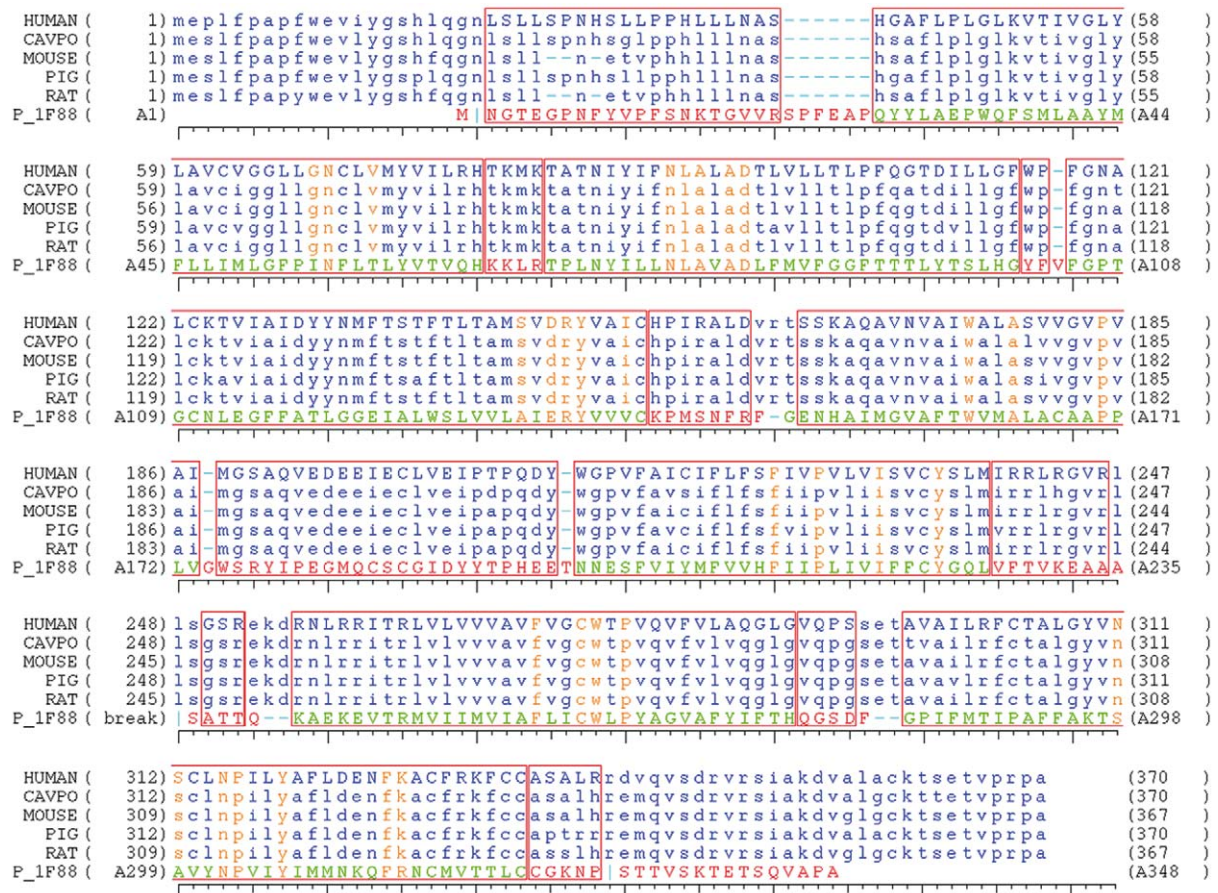


Figure 3. Multisequence alignment of the human ORL1-receptor (HORL) to bovine rhodopsin (P_1F88) and four other mammalian ORL1-receptor sequences, helices blue, loops green, pin-points orange.

Modelling the receptor protein

Initially, an alignment of the sequences of bovine rhodopsin (PDB: 1F88) [20] serving as template and the human ORL1-receptor (SwissProt P41146) was generated using the HOMOLOGY module within INSIGHT II [21]. For the first time, a receptor model of the ORL1-receptor was generated based on the crystal structure of bovine rhodopsin. The ORL1-receptor sequence shows an identity of 18% to the template. In order to support the positions of highly conserved amino acids four other ORL1-receptor sequences of mammalian species (guinea pig, mouse, pig, rat) showing high sequence identity (~94%) to the human ORL1-receptor were taken into account within a multiple sequence alignment (Figure 6).

The program PHDtm [22, 23] was used to predict the helices' lengths both for the ORL1-receptor and the rhodopsin sequence. Due to the according find-

ings by PHDtm, the lengths of the helical segments were adopted from the crystal structure (marked blue). Highly conserved amino acids analysed by the fingerprint approach developed by Baldwin [24] served as 'thumbtacks' (orange letters) for superimposing the ORL1-receptor sequence onto the available crystallographically derived 3D structure of bovine rhodopsin. Both the coordinates of the transmembrane helices (TM) and most of the loops (green) as well as the coordinates of the cysteines forming the conserved disulfide bridge were taken from the X-ray structure. The coordinates for remaining loop amino acids were assigned by searching the Brookhaven crystallographic database. Sidechain conformations that are not conserved in the ORL1-receptor and in the crystal structure were assigned using the program SCWRL [25]. This program adds sidechains to a protein backbone based on a backbone-dependent rotamer library.

Subsequently, the model was energetically minimised employing the conjugate gradient algorithm and subjected to a molecular dynamics simulation (MDS) (500 ps, distance dependent dielectric constant $\epsilon = 2r$, tether to backbone atoms = $250 \text{ kcal}\cdot\text{mol}^{-1}\cdot\text{\AA}^{-2}$) using the consistent valence force field (CVFF). The system was subjected to physiological conditions (pH = 7.4), so every acidic and basic amino acid was considered to exist in the charged state. A representative structure was chosen by using the program NMRCCLUS [26]. After subsequent energy minimization the steric quality of a modelled structure, i.e. the accuracy of geometric parameters such as bond lengths, bond angles, torsion angles and correctness of the amino acid chiralities has to be checked. Hence, the program PROCHECK [27] was applied, which automatically checks all these structural properties. The Ramachandran plot [27] (Figure 8) represents the main chain torsion angles ϕ and ψ , the major relevant indication for the structural quality of the ORL1-receptor.

Docking

In order to dock the ligands into their binding sites within the receptor model, FlexX [28], a fully automatic docking tool for flexible ligands, was used. The program needs the three-dimensional structure of the target protein and the accurately defined active site in a separate pdb-file. This method consists of three steps: the selection of a part of a molecule, the base fragment, the placement of the base fragment into the active site of a protein, and the subsequent reconstruction of the complete drug molecule by linking the remaining components step by step. For placing base fragments, two algorithms are in use. The first one superposes triples of interaction centers of a base fragment with triples of compatible interaction points in the active site. If a base fragment has fewer than three interaction centers or if the number of placements is too low, the second algorithm, called line matching, is started. This one matches pairs of interaction centers with pairs of interaction points. Because of geometry ambiguity, multiple placements are generated by rotation around the axis defined by the interaction points and centers. Both base placement algorithms generated a large number of solutions. A reduction by clash tests and clustering follows. Ranking the docking results is performed with a modification of the scoring function by Böhm [29, 30]. Algorithms and scoring function are described in more detail elsewhere [28–31].

Results and discussion

Pharmacophore

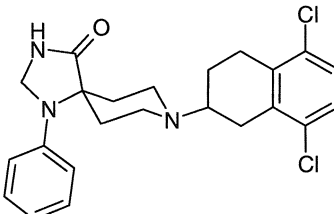
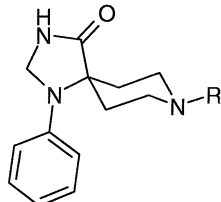
Based on a set of biologically characterized compounds, a ligand-based study was performed. For this purpose, a consistent set of agonists, notably substituted 1-phenyl-1,3,8-triaza-spiro[4.5]decan-4-ones, was taken from literature. The series of analogues was described by Hoffmann-La Roche with respect to their binding capacities to the human (Table 1a, 1b) and rat ORL1-receptor (Table 2a, 2b), respectively. The alignment of both receptor sequences shows a total identity of 94%, while the sequence identity within helical regions is about 98%. Moreover, the differences within the helical domains are of minor importance: Three valine residues in the human sequence are substituted by isoleucines in the rat sequence. In addition, the sidechains of the different amino acids face the membrane and have no influence on the putative binding pocket. As comparable binding data are prerequisite for the subsequent 3D-QSAR study, the binding affinities derived at receptors from different origin had to be adjusted according to ligand **1** which was tested in both receptor systems. This procedure resulted in an extended dataset to derive a more stable 3D-QSAR model with high predictive power. The ligand numbering system was adopted from literature in order to avoid confusion.

For the pharmacophoric superposition, the semi-rigid selective ligand Ro 64-6198 ($\text{pK}_i = 9.41$) was chosen as a representative structure. Based on a molecular mechanics simulation in combination with experimentally derived X-ray data on substructures of Ro 64-6198, a reference conformation was generated (Figure 2). Subsequently, FlexS was used to superimpose the remaining agonists automatically with the given reference. In Figure 4 the superposition of all investigated ligands is shown. Within the superposition only low energy conformations were taken into account. The basic nitrogens and atoms capable to form H-bonds were overlaid as well as the lipophilic regions. This superimposition of ligands highlights the spatial arrangement of structural features enabling molecules to bind selectively at the ORL1-receptor.

Ligand-based 3D-QSAR model

The above mentioned pharmacophore model provides information on the potential bioactive conformation of the ligands and the relative mutual orientation of the pharmacophoric groups. For further verification

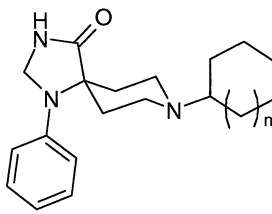
Table 1. Investigated ligand dataset, binding affinities (K_i) for human ORL1-receptor and opioid receptors (μ , κ , δ).

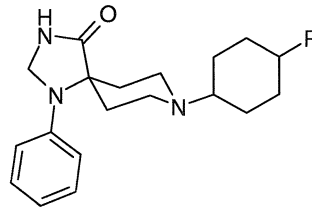
						
		$K_i(\pm\text{SEM})$ [nM]				
Compound		hORL1	μ	κ	δ	
1g (<i>S</i>)		2.8 (0.9)	5.9 (2.6)	40.1 (8.0)	415 (74)	
1h (<i>R</i>)		20.7 (7.8)	8.4 (2.2)	47.3 (7.8)	587 (30)	
						
		$K_i(\pm\text{SEM})$ [nM]				
Compound	R	hORL1	rORL1	μ	κ	δ
1m	2-indanyl	2.5	–	26.0 (0.6)	161	710
1n (<i>S</i>)	1-tetralinyl	10.2 (3.7)	–	13.3 (4.6)	17	nd
1o (<i>R</i>)	1-tetralinyl	2.5 (1.3)	–	12.3 (2.6)	46.3 (5.2)	530 (160)
Ro 64-6198 (1 <i>S</i> , 3 <i>aS</i>)	hexahydro-phenalenyl	0.39	–	47	89	1380
1 (<i>R</i>)	acenaphthenyl	0.25	0.41	4.0	20	100

of these qualitative findings, a 3D-QSAR study of the 25 ligands with a pK_i range from 6.4 to 10.3 has been performed using the GRID/GOLPE method. 3D-QSAR studies attempt to generate a correlation between physicochemical characteristics of the molecules and the experimentally derived binding affinities. Interaction energy values were calculated by the program GRID and resulted in 8722 data points. After the advanced pretreatment the data set still contains 7556 variables. The subsequent variable selection procedures and the final FFD selection resulted in 491 variables with major improvement of the quality of the model. The analysis yielded a correlation coefficient with a cross-validated q^2_{LOO} of 0.86. The respective conventional r^2 value amounts to 0.98. This means that the model explains more than 98% of the variance in ligand binding of the investigated compounds. The model is also robust, indicated by a high correl-

ation coefficient of $q^2 = 0.81$ obtained by using the leave-20%-out cross-validation procedure. These results (summarized in Table 3) underline a reasonable predictive power of the model. In Figure 5 the correlation between the predicted binding affinities and the experimentally determined affinities is shown; in Table 4 the numerical values of the results are listed. Compound **2h**, the ligand with the lowest affinity is the only outlier in the correlation. It is a common finding for molecules that are chemically different from all the other compounds in the dataset and are low or high affinity ligands to be overestimated or underestimated, respectively [14]. In Figure 6, the PLS coefficient map is displayed. The coefficient map indicates those areas in which the model has found a high correlation between the ligand-probe interaction energy and the biological activity. Thus, areas containing negative coefficients (cyan coloured) contribute to an increase in the activity. In contrast, an area with

Table 2. Investigated ligand dataset, binding affinities (K_i) for rat ORL1-receptor and opioid receptors (μ , κ , δ).

							
Compound	n	$K_i(\pm\text{SEM})$ [nM]					δ
		rORL1	hORL1	μ	κ	(adjusted K_i)	
2a	1	25	16	158	100	nd	
2b	2	4.7	3.1	51	12	>2000	
2c	3	1.9	1.3	13	9.1	>200	
2d	4	0.24	0.16	3.2	3.9	>200	
2e	5	0.082	0.05	0.66	2.1	46	
2f	6	0.49	0.32	0.21	0.82	15	
2g	7	0.95	0.63	0.28	2.9	570	
2h	10	600	398	nd	nd	nd	

							
Compound	R	Stereo	$K_i(\pm\text{SEM})$ [nM]				
			rORL1	hORL1	μ	κ	δ
(adjusted K_i)							
2i	Me	trans	41	25	nd	nd	nd
2j	Pr	trans	52	32	nd	nd	nd
2k	<i>i</i> -Pr	trans	4.6	2.8	8.3	31	670
2m	<i>t</i> -Bu	trans	12	7.4	nd	nd	nd
2n	Chx	trans	320	200	nd	nd	nd
2o	Me	cis	7.1	4.4	64	57	>2000
2p	Pr	cis	2.0	1.2	7.3	57	>540
2q	<i>i</i> -Pr	cis	0.079	0.049	3.2	26	242
2r	<i>t</i> -Bu	cis	3.3	2.0	6.7	38	450
2s	Chx	cis	1.5	1.0	1.5	29	330

positive coefficients (yellow) produces a decrease in the activity.

A further validation method, the scramble test was applied. Ten PLS models with scrambled pK values were generated. The characteristics of the resulting model are shown in Table 5. Surprisingly, every PLS

model yielded a rather high r^2 value. In contrast to that, none of the models survived the cross validation that is indicated by small q^2 values spanning a range from -0.27 – 0.36 . Furthermore, the high SDEP values also emphasise that the method is able to generate good

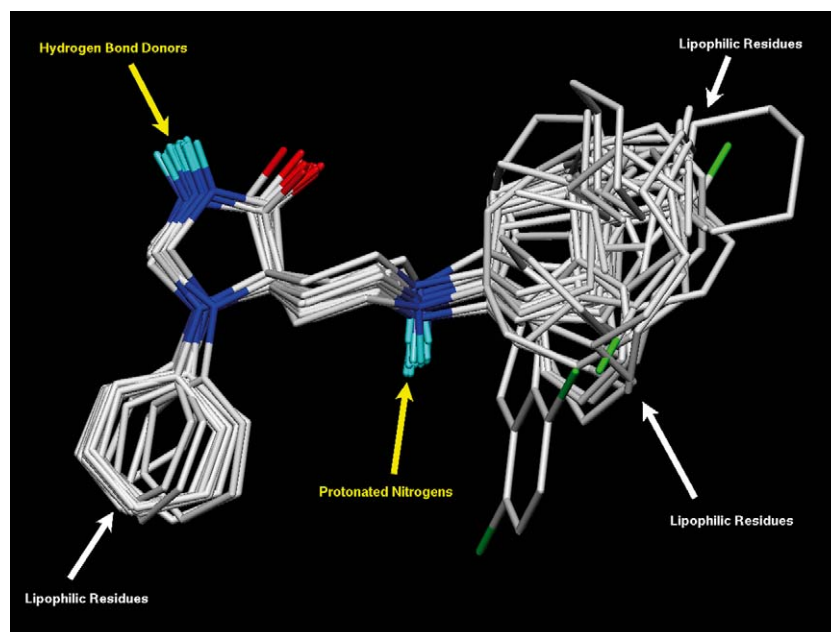


Figure 4. Results after ligand superposition employing FlexS; pharmacophoric descriptors are marked.

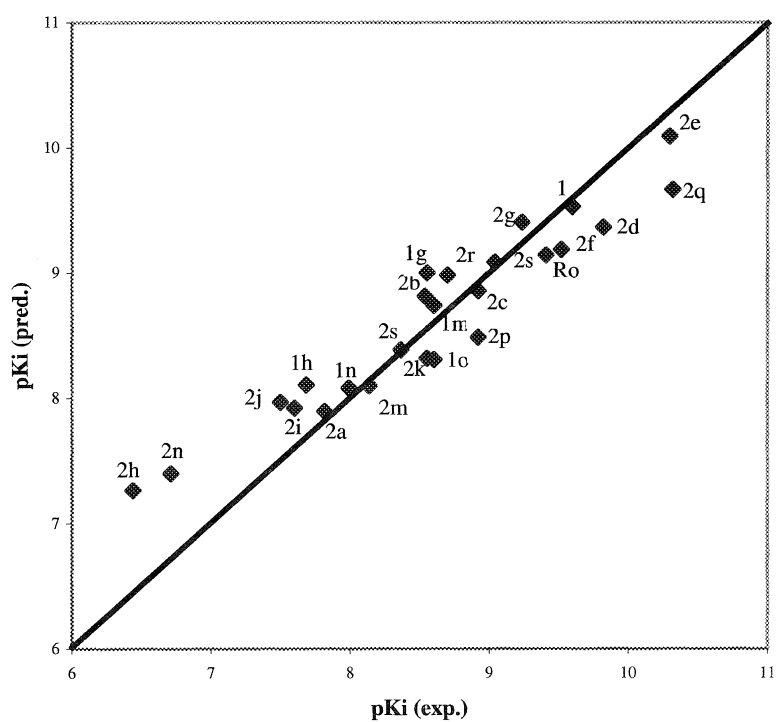


Figure 5. Cross-validated QSAR-model, leave one out, three LV's.

Table 3. Results of the 3D-QSAR study (ligand based).

	LOO	L20%O
LV's*	3	3
r^2	0.98	0.98
q^2	0.86	0.81
SDEP**	0.36	0.42

*LV's = Latent Variables.

**SDEP = Standard Deviation of the Error of Prediction.

Table 4. Results of the 3D-QSAR study (ligand based): list of experimental and predicted pK_i values, three LV's.

Compound	Experimental pK_i	Predicted pK_i
1	9.60	9.53
1g	8.55	9.00
1h	7.68	8.11
1m	8.60	8.74
1n	7.99	8.08
1o	8.60	8.31
2a	7.82	7.90
2b	8.54	8.81
2c	8.92	8.85
2d	9.82	9.37
2e	10.30	10.09
2f	9.52	9.19
2g	9.24	9.41
2h	6.44	7.27
2i	7.60	7.92
2j	7.50	8.00
2k	8.55	8.32
2m	8.14	8.10
2n	6.71	7.40
2o	8.37	8.39
2p	8.92	8.49
2q	10.32	9.67
2r	8.70	8.98
2s	9.04	9.09
Ro 64-6198	9.41	9.14

models only if binding affinities have been correctly assigned.

Receptor model

Following these ligand-based studies, a 3D model of the human ORL1-receptor was built based on the crystal structure of bovine rhodopsin [20] employing the

software Insight II [21]. The generated model was energetically minimised. Subsequently the receptor protein model was subjected to a MDS (500 ps). The energy deviations were observed during the term and after 300 ps, the receptor model reached an equilibrated state (Figure 7).

A representative structure was chosen from the equilibrated section of the MDS by NMRCCLUST [26] and minimised subsequently. The resulting protein conformations were analysed for structural violations. To verify the stereochemical quality of a modelled structure, the program PROCHECK [27] that automatically checks all stereochemical properties was used. The Ramachandran plot for the ORL1-receptor model is shown in Figure 8. A model of a protein structure of high quality is achieved when > 90% of the residues are found within the most favoured regions of the resulting Ramachandran plot. In case of the ORL-1 model structure, only 82% are found within that region. However, it has to be noted that (i) the receptor model does also contain the very flexible loop and terminal areas, and (ii) the amino acids occupying disallowed regions (His-42, Phe-115, Ile-156, Asp-195, Ala-336) are located in regions that are remote from the binding pocket, mainly in the loop regions.

Figure 9 shows the ORL1-receptor model superimposed with the crystal structure of bovine rhodopsin. Secondary structural elements are represented by red tubes (α -helices) and yellow arrows (β -strands). The β -strands in the N-terminus and the second extracellular loop form β -sheets that remained stable in the course of the MDS. These characteristics also occur in the crystal structure.

Docking

The compounds described above were tested for their competitive activity towards the radioligand nociceptin. A site-directed mutagenesis study with nociceptin has shown that Asp-130 in TM III is a crucial anchoring point for the physiological agonist [32]. This negatively charged amino acid should be an ideal counterpart for the basic nitrogen in the piperidine ring for forming a salt bridge. Consequently, Asp-130 was defined as an anchor residue.

For the manual docking procedure, ligand Ro 64-6198 in its pharmacophoric conformation was positioned between TM 3, 5, 6, and 7 at the head of the receptor from extracellular view. The ligand-receptor complex was energetically minimised and subjected to MDS (Figure 10). Control of the energy deviations in

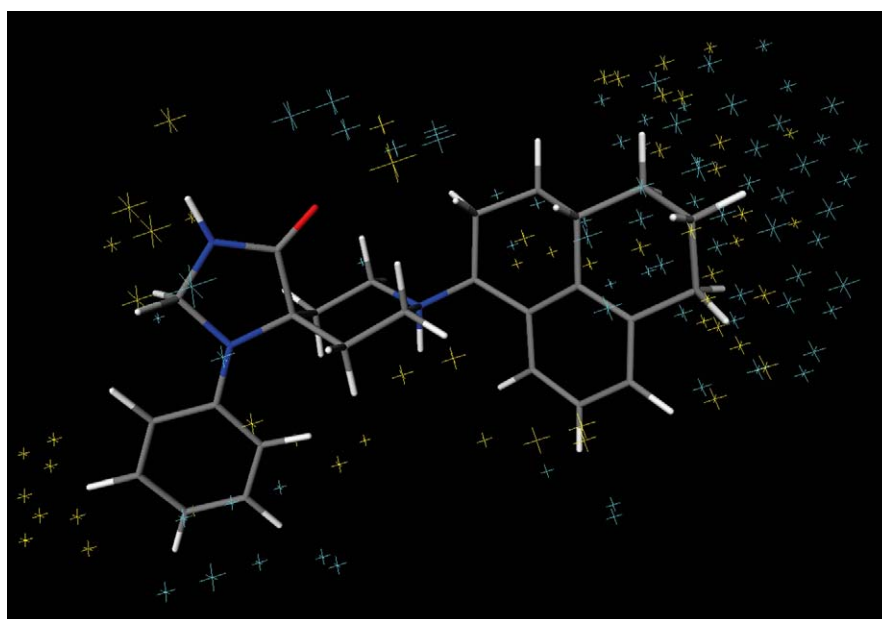


Figure 6. PLS coefficient map obtained using the phenolic OH-probe; the coefficients are represented by crosses; the cross sizes are proportional to their absolute value; negative coefficients are represented in cyan (cut-off ≤ -0.0036), positive coefficients are represented in yellow (cut-off $\geq +0.0036$); compound Ro 64-6198 is displayed for reference.

Table 5. Characteristics of the PLS models at three LV's after scrambling binding affinities.

Model	r^2	q^2	SDEP
1	0.80	0.13	0.90
2	0.84	-0.27	1.09
3	0.88	0.05	0.94
4	0.83	0.20	0.86
5	0.90	0.002	0.96
6	0.87	0.22	0.85
7	0.86	0.25	0.83
8	0.92	0.08	0.93
9	0.93	0.36	0.77
10	0.93	0.35	0.78

the course of the simulation shows that the complex reaches an equilibrated state (Figure 11). The salt-bridge between the protonated piperidine-nitrogen and Asp-130 remained stable. Additionally, an H-bond is formed between the hydrogen of the amide nitrogen of the agonist and the oxygen of Thr-305, resulting in two hydrophilic interaction points. On the other side, the lipophilic cavity consisting of Ile-127, Tyr-131, Met-134, Phe-135, Ile-204, Phe-215, Ile-219, Phe-220, Phe-224, Phe-272, Trp-276, Val-279, Val-283 stabilizes the compound in the binding pocket by

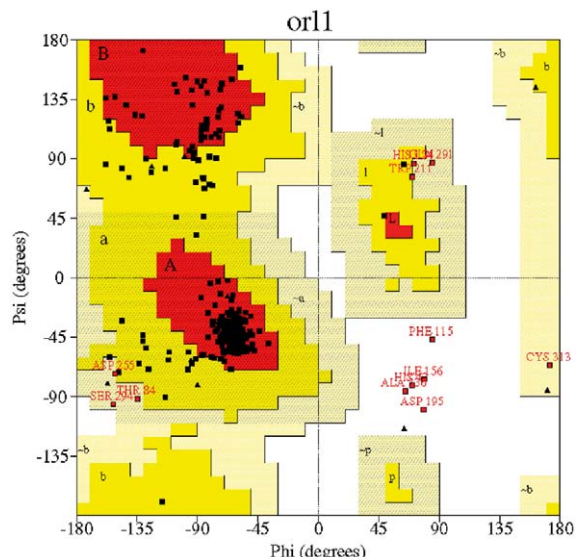
dispersive interactions with the aromatic moieties of the ligand.

The resulting conformation of Ro 64-6198 (i) after ligand based analysis (red) and (ii) the manual docking conformation (green) were overlaid (Figure 12). No major difference could be identified.

In order to support these results, the ligands were also docked into the active site of the receptor protein employing the docking program FlexX. The same interactions were found by the automatic docking routine for every compound (Figure 13).

Summarizing, for a ligand with high affinity and selectivity for the ORL1-receptor, an H-bond donor or acceptor in addition to NH^+ i.e. an amide group is a prerequisite, and a lipophilic residue is required within close proximity for hydrophobic interactions. The size of this lipophilic substituent including the linkage to the piperidine ring should not exceed 6.5 Å. Thr-305 and the mainly aromatic amino acids of the lipophilic part of the pocket seem to be responsible for the selectivity versus the opioid receptors, which differ from the ORL1-receptor as follows: (i) at position 305, the opioid receptors display a leucine, a lipophilic amino acid, instead of a threonine with an H-bond donating/accepting side chain; (ii) moreover, the lipophilic amino acids within the binding pocket of the opioid receptors are of smaller size and are more

flexible aliphatic residues compared with the aromatic cavity of the ORL1-receptor. Therefore, ligands with larger hydrophobic substituents at the piperidine ring show higher affinities for the classic opioid receptors.



These investigations on the receptor protein, the putative binding pocket, and the potential binding mode of ORL1-receptor agonists should be compared with the pharmacophore model. The receptor-based superposition bears a striking resemblance to the pharmacophoric superposition (Figure 14). Only small differences resulted in that comparison because of the limited cavity available for the lipophilic part of the ligands complexed with the receptor. Apart from that, the conformations resulting from the automated docking routine of FlexX are in agreement with the pharmacophore.

In order to compare NNC 63-0532 with the Hoffmann-La Roche agonists, the compound was manually and automatically docked into the binding site. For NNC 63-0532 the same interactions points are found by FlexX, i.e. Asp-130 and Thr-305, as well as the lipophilic pocket. The carbonyl group of the amide interacts with Thr-305 (Figure 16). For that



Figure 10. Receptor-ligand complex after manual docking procedure, side-view, top: extracellular side, bottom: intracellular side.

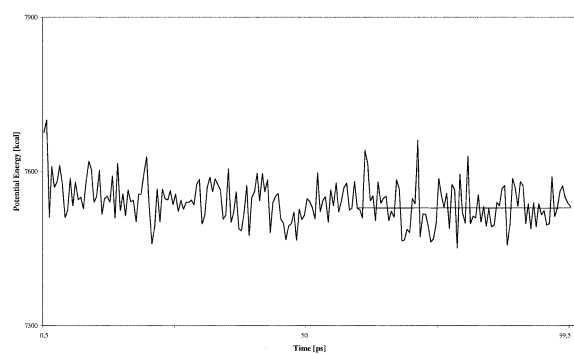


Figure 11. Energy development during the MDS of the receptor protein complexed with ligand Ro 64-6198; simulation time: 100 ps; the complex reaches an equilibrated state after 60 ps.

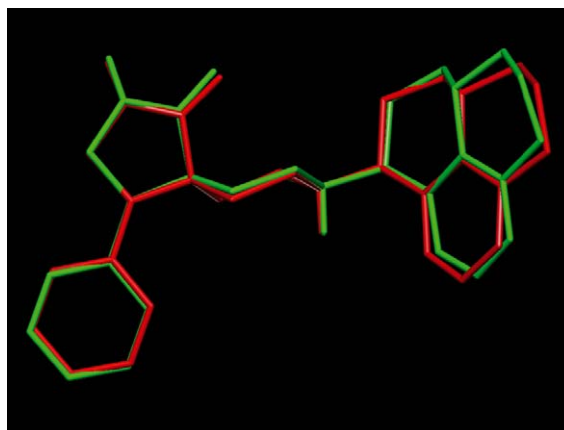


Figure 12. Red: Ro 64-6198 after ligand based analysis; green: Ro 64-6198 after manual docking procedure.

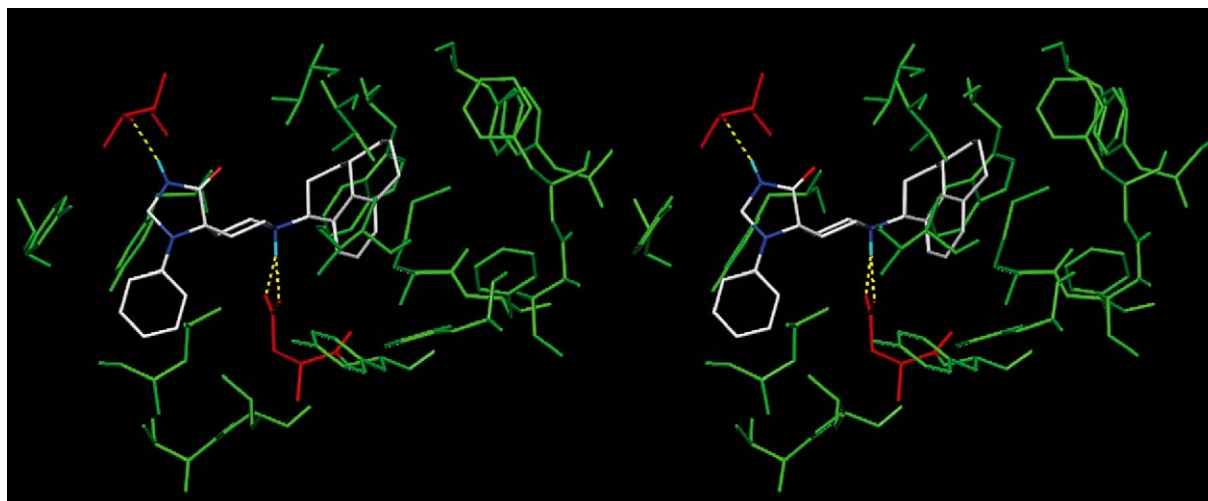


Figure 13. Stereoview of Ro 64-6198 docked into the binding site by FlexX; red: Asp-130 forming a salt bridge to the protonated piperidine nitrogen, Thr-305 forming an H-bond with NH of the amide; green: lipophilic contacts.

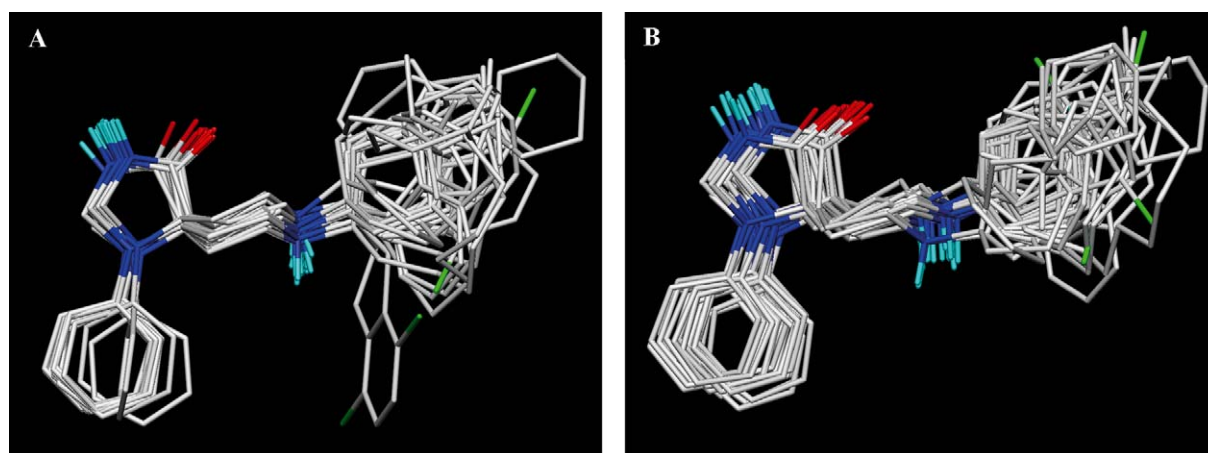


Figure 14. A: Ligand superposition after ligand based analysis (FlexS); B: Ligand conformations after automated docking with FlexX.

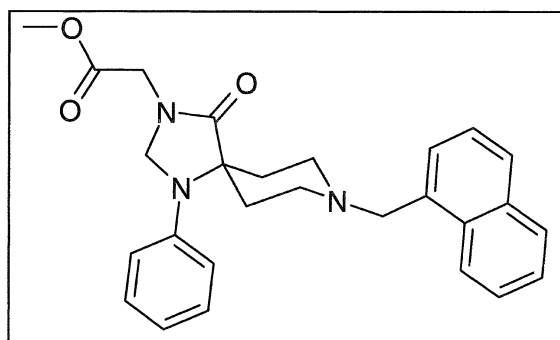


Figure 15. NNC 63-0532.

reason, NNC63-0532 shows basically the same affinity for the ORL1-receptor as e.g. ligand **1o** that

exhibits high similarity to NNC63-0532. The three-fold lack of binding strengths might be due to bad steric contacts.

The main structural difference between both molecules is given by the substituent of the amide nitrogen. Therefore, the affinity of NNC 63-0532 would increase if receptor amino acids capable to function as H-bond donors were available. However, in the relevant region of the receptor primarily lipophilic residues (Ile-54, Ala-306) are found; for that reason no favourable interactions can be formed. Consequently, an H-bond accepting substituent like the acetic acid methyl ester at the amide is not able to bind stronger at the ORL1-receptor. Assumingly affinity would in-

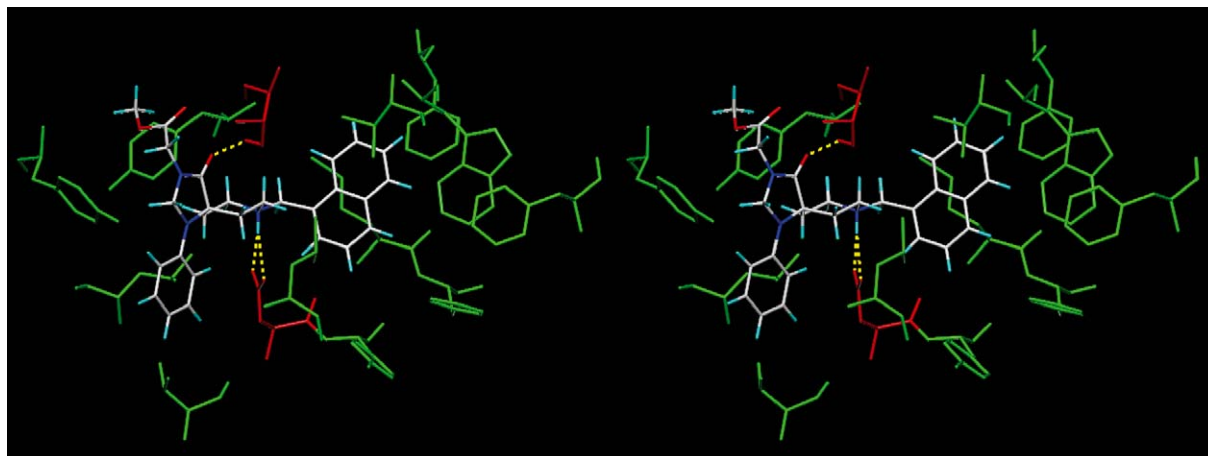


Figure 16. Stereoview of NNC 63-0532 automatically docked into its binding pocket by FlexX; red: Asp-130 forming a salt bridge to the protonated piperidine nitrogen, Thr-305 interacts with the carbonyl group of the amide; green: lipophilic contacts.

crease if the ester substructure was replaced by a lipophilic fragment.

Early in 2003, when this manuscript already was in preparation, Hoffmann-La Roche published a dataset of new non-peptide agonists containing a slightly altered scaffold compared to the molecules investigated within this work [34]. The new compounds were probed for compliance with the developed pharmacophore model and the proposed binding pocket. Examinations of the conformational space and superposition of the new ligands with Ro 64-6198 using FlexS showed an excellent concordance with the results of the ligand-based investigations. After molecular dynamic simulations of the receptor model complexed with two representatives (enantiomers) of the new dataset, the molecules seemed to fit in the assumed binding site. Only a minor deviation within the binding mode of the two enantiomers occurred during the MDS that might reflect the small difference of the binding affinity ($K_i = 0.55$ nM and 1.22 nM, respectively). Thus, these findings fully support our previous results. Additional investigations will be performed in more detail and will be an essential part of a further publication.

Within this study, a receptor model for the ORL1-receptor was generated based on the crystal structure of bovine rhodopsin. The proposed binding pocket for ORL1-receptor agonists that was analysed independently from previous molecular modelling investigations of the ORL1-receptor [35] overlaps with the assumed nociceptin binding site. The N-terminal hydrophobic domain (FGGF) of the physiological ligand is supposed to bind inside the helix bundle between TM

3, 5, 6, and 7 [35, 36]. Alanine mutation of Asp-130 and Tyr-131 in TM3, Phe-220 and Phe-224 in TM5, and Trp-276 in TM6 yielded mutant receptors with reduced affinity, and proportionally decreased reactivity towards nociceptin. In a previous molecular modelling study (1998), a receptor model of the ORL1-receptor applying the bovine rhodopsin model of Herzyk and Hubbard (1995) [37] as template was generated and complexed with nociceptin, the physiological 17 AS comprising neuropeptide [35]. The aromatic residues were assumed to form hydrophobic cavities for the Phe-sidechains, Asp-130 ionically interacted with the positively charged N-terminus. These amino acids that are presumed to be essential for the nociceptin binding are also supposed to interact with the non-peptide agonists. A salt bridge between Asp-130 and the basic nitrogen is formed and lipophilic interactions are generated between the aromatic amino acids and the lipophilic moieties of the ligands as well. Summarising, it may be concluded that the results of our investigations on the binding site of non-peptide agonists are favourably supported by the present data. The small molecules might interact with the same amino acids that are essential for binding of the physiological agonist.

Conclusions

The presented study was initiated to explore the 3D structure of the ORL1-receptor and the interaction of ORL1-receptor selective ligands with their receptor. A ligand-based pharmacophore model of 25 ORL1-

receptor selective agonists has been proposed. After analysing the conformational space of one ligand with a small number of rotatable bonds, the remaining molecules were overlaid automatically onto this reference by superimposing important pharmacophoric points. The three-dimensional arrangement of structural features important for interacting with the target protein is shown. Additionally, the results of the superposition were supported by 3D-QSAR studies that resulted in a model with high predictive power, indicated by high cross-correlation coefficients.

Further, a three-dimensional structural model of the ORL1-receptor using homology modelling techniques was constructed and subjected to MDS. The resulting protein model that showed a good steric quality was used to dock a series of analogues into the putative binding site. A crucial anchoring point constituted by Asp-130 was the starting position for a manual docking procedure. The protonated nitrogen of the piperidine should form a salt bridge to the negatively charged aspartate. Apart from this interaction, an H-bond is formed between the oxygen within the sidechain of Thr-305 and the hydrogen of the amide nitrogen. Furthermore, a net of lipophilic residues delineates the binding pocket. Results of automatic docking operations supported the assumed orientation of the ligands inside their binding site since the program found the same interacting partners for the compounds.

In summary, these findings indicate the structural requirements for potent and selective ORL1-receptor agonists. Further investigations on a new dataset of ligands [34] will serve to gain new insights into the molecular details of the ligand binding event at the ORL1-receptor and may result in the future in new concepts for the design of potent and selective non-peptide ORL1-receptor agonists. On this account, the protein model, particularly the proposed binding pocket will be applied for virtual screening methods in order to gain information about putative ligands. The scoring function implemented in FlexX/ FlexX-Pharm [38] and subsequent 3D-QSAR studies will be utilised to evaluate the results.

References

1. Mollereau, C., Parmentier, M., Mailleux, P., Butour, J.-L., Moisand, C., Chalon, P., Caput, D., Vassart, G. and Meunier, J.-C., *FEBS Lett.*, 341 (1994) 33.
2. Ronzoni, S., Peretto, I. and Giardina, G., *Exp. Opin. Ther. Patents*, 11 (2001) 525.
3. Meunier, J.C., *Eur. J. Pharmacol.*, 340 (1997) 1.
4. Meunier, J.C., *Exp. Opin. Ther. Patents*, 10 (2000) 371.
5. Reinscheid, R.K., Nothacker, H.-P., Boursion, A., Ardati, A., Henningsen, R.A., Bunzow, J.R., Grandy, D.K., Langen, H., Monsma, F.J., Jr. and Civelli, O., *Science*, 270 (1995) 792.
6. Jenck, F., Wichmann, J., Dautzenberg, F.M., Moreau, J.-L., Ouagazzal, A.M., Martin, J.R., Lundstrom, K., Cesura, A.M., Poli, S.M., Röver, S., Kolczewski, S., Adam, G. and Kilpatrick, G., *Proc. Natl. Acad. Sci. USA*, 97 (2000) 4938.
7. Röver, S., Adam, G., Cesura, A.M., Galley, G., Jenck, F., Monsma, F.J., Jr., Wichmann, J. and Dautzenberg, F., *J. Med. Chem.*, 43 (2000) 1329.
8. Röver, S., Wichmann, J., Jenck, F., Adam, G. and Cesura, A.M., *Bioorg. Med. Chem. Lett.*, 10 (2000) 831.
9. Weiner, S. J., Kollman, P.A., Case, D.A., Singh, U.C., Ghio, C., Alagona, G., Profeta, S. and Weiner, P.J., *J. Am. Chem. Soc.*, 106 (1984) 765.
10. FlexS: Lemmen, C., Lengauer, T. and Klebe, G., *J. Med. Chem.*, 41 (1998) 4502.
11. Lemmen, C. and Lengauer, T., *J. Comput.-Aided Mol. Des.*, 11 (1997) 357.
12. GRID, Version 20, Molecular Discovery Ltd., Oxford, UK.
13. GOLPE 4.5. Multivariate Infometric Analysis Srl., Perugia, Italy, 1999.
14. Cruciani, G. and Watson, K.A., *J. Med. Chem.*, 37 (1994) 2589.
15. Pastor, M., Cruciani, G. and Clementi, S., *J. Med. Chem.*, 40 (1997) 1455.
16. Baroni, M., Constantino, G., Cruciani, G., Riganelli, D., Valigli, R. and Clementi, S., *Quant. Struct.-Act. Relat.*, 12 (1993) 9.
17. Oprea, T.I. and Garcia, A.E., *J. Comput.-Aided Mol. Des.*, 10 (1996) 186.
18. Krystek, S.R., Hunt, J.T., Stein, P.D. and Stouch, T.R., *J. Med. Chem.*, 38 (1995) 659.
19. Höltje, H.-D., Sippl, W., Rognan, D. and Folkers, G., *Molecular Modeling: Basic Principles and Applications*, 2nd edition, Wiley-VCH Verlagsgesellschaft, Weinheim, Germany, 2003.
20. Palczewski, K., Kumasaka, T., Hori, T., Behnke, C.A., Motoshima, H., Fox, B.A., Le Trong, I., Teller, D.C., Okada, T., Stenkamp, R.E., Yamamoto, M. and Miyano, M., *Science*, 289 (2000) 739.
21. Insight II 2000, Accelrys Inc., San Diego, CA.
22. Rost, B., Casadio, R., Fariselli, P. and Sander, C., *Protein Sci.*, 4 (1995) 521.
23. Rost, B., Fariselli, P. and Casadio, R., *Protein Sci.*, 5 (1996) 1704.
24. Baldwin, J.M., Schertler, G.F.X. and Unger, V.M., *J. Mol. Biol.*, 272 (1997) 144.
25. SCWRL: Dunbrack, R.L. and Cohen, F.E., *Protein Sci.*, 6 (1997) 1661.
26. NMRCLUST: Kelley, L.A., Gardner, S.P. and Sutcliffe, M.J., *Protein Eng.*, 9 (1996) 1063.
27. PROCHECK: Laskowski, R.A., MacArthur, M.W., Moss, D.S. and Thornton, J.M., *J. Appl. Crystallogr.*, 26 (1993) 283.
28. FlexX: Kramer, B., Rarey, M. and Lengauer, T., *Proteins*, 37 (1999) 228.
29. Böhm, H.-J., *J. Comput.-Aided Mol. Des.*, 6 (1992) 593.
30. Böhm, H.-J., *J. Comput.-Aided Mol. Des.*, 8 (1994) 243.
31. Rarey, M., Kramer, B. and Lengauer, T., *J. Comput.-Aided Mol. Des.*, 11 (1997) 369.
32. Mouldous, L., Topham, C.M., Moisand, C., Mollereau, C. and Meunier, J.-C., *Mol. Pharmacol.*, 57 (2000) 495.

33. Thomsen, C. and Hohlweg, R., *Br. J. Pharmacol.*, 131 (2000) 903.
34. Kolczewski, S., Adam, G., Cesura, A.M., Jenck, F., Hennig, M., Oberhauser, T., Poli, S.M., Rössler, F., Röver, S., Wichmann, J. and Dautzenberg, F.M., *J. Med. Chem.*, 46 (2003) 255.
35. Topham, C.M., Mouledous, M., Poda, G., Maigret, B. and Meunier, J.-C., *Protein Eng.*, 11 (1998) 1163.
36. Meunier, J.-C., Mouledous, L. and Topham, C.M., *Peptides*, 21 (2000) 893.
37. Herzyk, P. and Hubbard, R.E., *Biophys. J.*, 69 (1995) 2419.
38. Hindle, S.A., Rarey, M., Buning, C. and Lengauer, T., *J. Comput.-Aided Mol. Des.*, 16 (2002) 129.